Basis Expansion Model for Fast Time-Varying Channel Estimation in High Mobility Scenarios

Xinlin Lai, Zhonghui Chen(✉), and Yisheng Zhao

College of Physics and Information Engineering, Fuzhou University, Fuzhou, China
xinlinlaifzu@163.com, {czh,zhaoys}@fzu.edu.cn

Abstract. In order to provide the users with reliable wireless communication service in high-speed mobility scenarios, we need to obtain channel state information by channel estimation. However, the wireless channel presents a characteristic of dynamic change in high-speed mobility environments. It will bring great challenge to channel estimation. Aiming at the high-speed railway communication system, the issue of the fast time-varying channel estimation is investigated in this paper. The impulse response of the fast time-varying channel is modeled as the product of the basis functions and the coefficients by introducing a basis expansion model (BEM). Meanwhile, the comb pilot clusters are inserted in frequency domain. The coefficients of basis functions are derived by the least-square estimation criterion so as to realize the estimation of the channel impulse response. Simulation results show that optimization generalized complex exponential BEM (OGCE-BEM) has the smallest normalized mean square error among the various types of BEMs.

Keywords: Fast time-varying channel · Channel estimation · Basis expansion model

1 Introduction

It is well known that the wireless channel is complex and variable. If the mobile terminal has high-speed mobility, it is more difficult to obtain the channel state information (CSI). For the long term evolution for railway (LTE-R) system [1], the speed of a train is more than 300 km per hour (km/h). The wireless channel is a frequency-time doubly selective fading channel, which presents a fast time-varying characteristic [2]. It will bring about serious inter-carrier interference, so the system performance will deteriorate severely. The communication system performance can be improved greatly if we obtain the CSI by channel estimation. Therefore, it is of great significance to conduct the research on channel estimation in LTE-R system.

Recently, the channel estimation issue has attracted extensive research attention. In [3], the authors present a blind channel estimation method by zero filling on the receiving data within a time block. It has high spectrum utilization and high data transmission efficiency. The authors of [4] propose that the sender

Q. Chen et al. (Eds.): ChinaCom 2016, Part I, LNICST 209, pp. 489–501, 2018.
DOI: 10.1007/978-3-319-66625-9_48

transmits a training sequence to update the current CSI at a periodic interval. Data symbols and training sequences are sent separately, and the training sequences are used to estimate the time-varying channel. Coleri et al. [5] compare the channel estimation schemes based on block pilot and comb pilot in orthogonal frequency division multiplexing (OFDM) system. According to the low-pass interpolation, a channel estimation strategy based on comb pilot is developed, which can acquire a high estimation precision. Both the cross correlation in time and frequency domains and the statistical characteristic of the fast fading diffuse wireless channel are fully taken into account in [6]. A channel estimation algorithm based on minimum mean square error is proposed, which can improve the estimation precision.

However, the blind channel estimation method need to use the statistics of the wireless channel. Therefore, it has a high computational complexity and a poor practicability. The channel estimation algorithm based on training sequence wastes a lot of bandwidth, which is suitable for slow changing channels only. Pilot-aided channel estimation strategy has the advantages of low complexity and high accuracy, and is fit to the fast time-varying channel [7]. Among various kinds of pilot-aided channel estimation strategies, the channel estimation strategy based on a basis expansion model (BEM) can well approximate the time-varying channel [8], which has drawn great attention. The representative BEMs are complex-exponential BEM (CE-BEM), generalized complex-exponential BEM (GCE-BEM), polynomial BEM (P-BEM), and so on. In [9], an oversampling technology is adopted to improve the performance of CE-BEM, which can increase the frequency resolution and reduce the estimation error on the edge of spectrum. The authors of [10] present a channel estimation algorithm by inserting the training sequence in the time domain. The channel impulse response of the training sequence is obtained first. Then, the channel impulse response of the useful data is fitted by using the P-BEM. In consequence, there is a strong motivation to investigate the fast time-varying channel estimation via the BEM in high-speed mobility scenarios.

In this paper, we employ BEM to discuss the dynamic changing channel estimation problem in the LTE-R system. Fast time-varying channel model is established by utilizing the BEM. The channel impulse response is expressed as the summation of several basis functions multiplied by the corresponding coefficients. Then we insert isometric comb pilot clusters in the frequency domain. The BEM coefficients are estimated based on the least-square (LS) estimation criterion with low computational complexity. Thus, the fast time-varying channel in high-speed mobility scenarios can be achieved approximately. In addition, we compare different BEMs by simulation in terms of the normalized mean square error (NMSE).

The remainder of this paper is arranged as follows. Section 2 describes the system model of high-speed railway communication scenarios. In Sect. 3, the fast time-varying channel estimation strategy based on BEM is presented. Some simulation results and discussions are shown in Sect. 4. In the end, conclusion and future work are given in Sect. 5.

2 System Model

The network architecture of the LTE-R communication system is shown in Fig 1. The coverage area of traditional mobile communication system is usually plane shape, while the coverage area of the high-speed railway communication system is belt shape. The dedicated network topology of LTE-R system is composed of building baseband unit (BBU) and radio remote unit (RRU). A BBU is connected to multiple RRUs by optical fiber, which is used to process baseband signal. Multiple RRUs are continuously and equidistantly deployed along the railway line, which are used to process radio frequency signal. A vehicular station (VS) is installed on the top of the first carriage, which is used to receive radio frequency signals from RRU. By using the cable and the repeater (R) in each carriage, the signals received by VS are sent to a user equipment (UE) in a certain carriage. It should be noted that the wireless channel between RRU and VS is estimated in the paper. In high-speed mobility scenarios, the wireless channel is frequency-time doubly selective fading channel, which will bring challenges to the channel estimation.

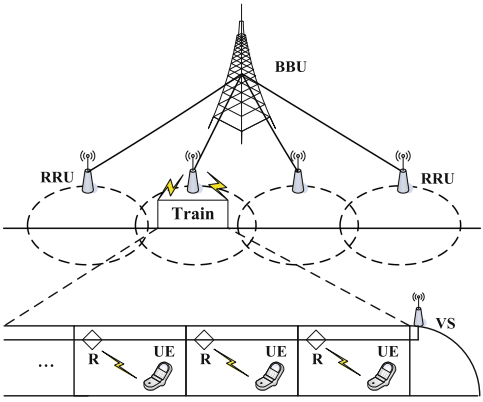

Fig. 1. Network architecture of high-speed railway communication system.

We assume that the RRU is sender, and the VS is the receiver. For the discrete time-varying multipath channel, the input signal and output signal in time-domain can be described as [11]: $y[n] = \sum_{l} h[n,l]x[n-l] + w[n]$, where $h[n,l]$ denotes the channel impulse response at the n-th moment on the l-th path, $x[n-l]$ is the sending signal at the $(n-l)$-th moment, and $w[n]$ indicates additive white Gaussian noise at the n-th moment.

For the LTE-R system, OFDM is one of key technologies. One OFDM symbol need to use N subcarriers. The signals carried by N subcarriers can be written as: $\mathbf{X} \triangleq (X[0], X[1], \cdots X[N-1])^T$, which represents the sending signal in frequency domain. Before sending the signal, we let the N subcarriers do N point

fast Fourier inverse transformation (IFFT). Then we get the time domain signal: $\mathbf{x} = (x[0], \cdots x[N-1])^T$. In order to suppress inter-symbol interference (ISI) of multipath channel effectively, we need to add cyclic prefix to the time domain signal at the sender, and remove the cyclic prefix at the receiver. Therefore, the received signal in time domain can be expressed as:

$$\mathbf{y} = \mathbf{H}\mathbf{x} + \mathbf{w} = (y[0], y[1], \cdots, y[N-1])^T, \tag{1}$$

where $\mathbf{H}$ is an $N \times N$ channel transfer matrix and similar to cyclic shift matrix [8]. The element of the i-th row and j-th column ($0 \leq i, j \leq N-1$) in the matrix is defined as:

$$\mathbf{H}[i,j] = \begin{cases} h[i, i-j] & (i \geq j) \cap (i-j < L) \\ h[i, i+N-j] & (i < j) \cap (i+N-j < L) \\ 0 & else \end{cases}. \tag{2}$$

At the receiver, the received signal in frequency domain can be expressed as:

$$\mathbf{Y} = \mathbf{F}\mathbf{y} = \mathbf{F}\mathbf{H}\mathbf{F}^H\mathbf{X} + \mathbf{F}\mathbf{w}, \tag{3}$$

where $\mathbf{Y} = (Y[0], Y[1], \cdots, Y[N-1])^T$ denote output signal in frequency domain. $\mathbf{w} = (w[0], w[1], \cdots, w[N-1])^T$ indicates noise signal in time domain. $\mathbf{F}$ is a standard normalized Fourier matrix [12]. As a result, the transfer matrix of the wireless channel in frequency domain can be written as: $\mathbf{G} = \mathbf{F}\mathbf{H}\mathbf{F}^H$. Thus, Eq. (3) can be simplified as: $\mathbf{Y} = \mathbf{G}\mathbf{X} + \mathbf{W}$.

3 Channel Estimation Strategy

In this section, the basis expansion model is introduced first. Then, the fast time-varying channel estimation strategy based on the basis expansion model is presented.

3.1 Basis Expansion Model (BEM)

For the multipath channel, the channel parameters in each path are changing all the time during an OFDM symbol. The number of channel parameters needed to be estimated is NL [5], which is usually very large. Here, N is the number of sampling points in an OFDM symbol and L represents the number of multipath. Therefore, the estimation of multipath channel cannot be realized directly.

BEM uses Q orthogonal basis functions to approximate the dynamic changes of the channel environment [7]. Then, the channel impulse response for the l-th path can be represented as: $\mathbf{h}_l = [h[0,l], h[1,l], \cdots, h[N-1,l]] (0 \leq l \leq L-1)$, $L \geq \lceil \tau_{\max}/T_s \rceil + 1$, where $\tau_{\max}$ denotes the maximum multipath delay and T_s is the sampling period. The q-th basis function vector is expressed as: $\mathbf{b}_q = (b[0,q], b[1,q], \cdots, b[N-1,q])^T (0 \leq q \leq Q-1)$, $Q \geq \lceil 2f_{\max} N T_s \rceil + 1$, where

$f_{\max}$ is the maximum Doppler frequency shift. Then, we use BEM to match the channel impulse response of the l-th path:

$$\mathbf{h}_l = \sum_{q=0}^{Q-1} c_q^l \mathbf{b}_q, \tag{4}$$

where $\mathbf{h}_l$ and $\mathbf{b}_q$ are both $N \times 1$ column vectors, and c_q^l denotes the coefficient of the l-th path and the q-th basis function. We rewrite Eq. (4) as matrix form: $\mathbf{h}_l = \mathbf{B}\mathbf{c}^l$. Here, $\mathbf{B}$ is an $N \times Q$ matrix. It consists of Q basis functions, which can be written as: $\mathbf{B} = [\mathbf{b}_0, \mathbf{b}_1, \cdots, \mathbf{b}_{Q-1}]$. Moreover, $\mathbf{c}^l$ is a $Q \times 1$ column vector. It consists of Q basis function coefficients of the l-th path, which is defined as: $\mathbf{c}^l = \left(c_0^l, c_1^l, \cdots, c_{Q-1}^l\right)^T$. According to BEM, the estimation of the time-varying channel impulse response is transformed into the estimation of the basis function coefficients. Therefore, the number of channel estimation is reduced from NL to QL.

Classical complex exponential BEM (CE-BEM) adopts Fourier basis as the basis functions [13]. The resolution of CE-BEM can not meet the requirements while modeling. Therefore, the estimation error on the edge of the spectrum is large. Moreover, discrete Fourier transform leads to spectrum leakage, so the estimation error of CE-BEM is not small enough.

GCE-BEM is an improvement of CE-BEM by using oversampling technique to reduce the sampling interval [9], which can effectively reduce the estimation error on the edge of spectrum caused by insufficient sampling points. The basis functions are defined as:

$$b_q(n) = e^{j2\pi \frac{q-\frac{Q-1}{2}}{KN} n}, \tag{5}$$

where Q meets the condition: $Q \geq \lceil 2f_{\max} KNT_s \rceil + 1$, and we set $K = 2$ generally. The frequency of basis functions is $f_q = (q - (Q-1)/2)/KNT_s$. The maximum frequency of GCE-BEM basis functions is $f_Q = (Q-1)/2KNT_s \geq \lceil f_{\max} \rceil$. Compared with CE-BEM, GCE-BEM has more high-frequency basis functions, whose frequencies are higher than $f_{\max}$. So it will be more susceptible to the effects of high frequency noise. As a result, the modeling error will be more obvious.

Optimization generalized complex exponential BEM (OGCE-BEM) is the result of a correction processing for the frequency of GCE-BEM basis functions. The basis functions are constructed as:

$$b_q(n) = e^{j2\pi g \frac{q-\frac{Q-1}{2}}{KN} n}, \tag{6}$$

where $g = 2Kf_{\max}N/(Q-1)$. The maximum frequency of the basis functions is $g \times (Q-1)/(2KN) = f_{\max}$. OGCE-BEM can remove the basis functions whose frequencies are higher than $f_{\max}$, which can effectively reduces the influence of Gaussian white noise and overcomes the problem of spectrum leakage in CE-BEM. Therefore, OGCE-BEM can approximate the real channel more accurately.

3.2 Fast Time-Varying Channel Estimation Strategy

We need to estimate the basis function coefficients of BEM. The main idea is: Firstly, we put the expression of BEM into the channel transfer function in time domain, and then transfer the channel transfer function to the frequency domain. Next, in order to solve the basis function coefficients simply, we separate the BEM coefficients completely. In the end, we can obtain the channel impulse response in time domain [8].

According to the Eq. (4), the channel impulse response for the l-th path and the q-th basis function can be seen as the linear superposition of Q basis functions at the n-th sampling moment, which can be written as: $h[n,l] = \sum_{q=0}^{Q-1} c_q^l b[n,q]$. Then, we put this expression into the channel transfer function in time domain:

$$\begin{aligned} y[n] &= \sum_{l=0}^{L-1} \sum_{q=0}^{Q-1} c_q^l b[n,q] x[n-l] + w[n] \\ &= \sum_{q=0}^{Q-1} b[n,q] \left\{ \sum_{l=0}^{L-1} c_q^l x[n-l] \right\} + w[n] \end{aligned}. \tag{7}$$

We rewrite the second accumulator of the second row in Eq. (7):

$$\sum_{l=0}^{L-1} c_q^l x[n-l] = \left(c_q^{L-1}, \cdots, c_q^0\right) \begin{pmatrix} x[n-L+1] \\ \vdots \\ x[n] \end{pmatrix}. \tag{8}$$

In order to facilitate the transformation, we define a matrix: $\Lambda_q^b = diag\{\mathbf{b}_q\}$. Λ_q^b is an $N \times N$ diagonal matrix, which consists of N elements of column vector $\mathbf{b}_q$. We can write Eq. (7) as vector form:

$$\mathbf{y} = \sum_{q=0}^{Q-1} \Lambda_q^b \mathbf{C}_q \mathbf{x} + \mathbf{w}, \tag{9}$$

where $\mathbf{C}_q$ is an $N \times N$ standard cyclic matrix. Each column of $\mathbf{C}_q$ consists of L BEM coefficients of the q-th basis function, which can be written as:

$$\mathbf{C}_q = \begin{pmatrix} c_q^0 & 0 & \cdots & c_q^{L-1} & \cdots & c_q^1 \\ c_q^1 & c_q^0 & \cdots & \cdots & c_q^3 & c_q^2 \\ c_q^2 & c_q^1 & c_q^0 & \ddots & \ddots & \vdots \\ \vdots & \ddots & \ddots & \ddots & \vdots & \vdots \\ 0 & \cdots & \ddots & \ddots & c_q^0 & 0 \\ 0 & \cdots & c_q^{L-1} & \cdots & c_q^1 & c_q^0 \end{pmatrix}. \tag{10}$$

The distribution of $\mathbf{C}_q$ is consistent with the channel transfer matrix $\mathbf{H}$. Then we apply Fourier transform to both sides of Eq. (9). For the purpose of facilitating

the extraction of the basis functions coefficients, we define a column vector: $\mathbf{c}_q = \left(c_q^0, c_q^1, \cdots, c_q^{L-1}\right)^T$. Therefore, the wireless channel model is transferred to the frequency domain:

$$\begin{aligned}\mathbf{Y} = \mathbf{F}\mathbf{y} &= \sum_{q=0}^{Q-1} \mathbf{F}\Lambda_q^b \mathbf{F}^H \mathbf{F}\mathbf{C}_q \mathbf{F}^H \mathbf{F}\mathbf{x} + \mathbf{F}\mathbf{w} \\ &= \sum_{q=0}^{Q-1} \mathbf{D}_q \boldsymbol{\Delta}_q \mathbf{X} + \mathbf{W} = \mathbf{H}^{\nabla}\mathbf{X} + \mathbf{W}\end{aligned}, \tag{11}$$

where $\mathbf{D}_q = \mathbf{F}\Lambda_q^b\mathbf{F}^H = \mathbf{F}diag\left\{\mathbf{b}_q\right\}\mathbf{F}^H$ and $\boldsymbol{\Delta}_q = \mathbf{F}\mathbf{C}_q\mathbf{F}^H = \sqrt{N}diag\left\{\mathbf{F}^L\mathbf{c}_q\right\}$. To observe the Eq. (11), we can find that: $\mathbf{D}_q$ is an $N \times N$ matrix but not a diagonal matrix. The distribution shape of nonzero elements in the matrix is banded and along with the diagonal. Then we transfer $\mathbf{C}_q$ into the frequency domain. And then, we obtain $\boldsymbol{\Delta}_q$, which is an $N \times N$ diagonal matrix. $\mathbf{F}^L$ is an $N \times L$ matrix, which consists of the first L columns of the standard normalized Fourier matrix. Next, we use matrix switching law to realize the following conversion:

$$\boldsymbol{\Delta}_q\mathbf{X} = \sqrt{N}diag\left\{\mathbf{F}^L\mathbf{c}_q\right\}\mathbf{X} = \sqrt{N}diag\left\{\mathbf{X}\right\}\mathbf{F}^L\mathbf{c}_q = \hat{\mathbf{X}}\mathbf{c}_q\,, \tag{12}$$

where $\mathbf{X}$ and $\mathbf{F}^L\mathbf{c}_q$ are both $N \times 1$ column vectors. We define $\hat{\mathbf{X}} = \sqrt{N}diag\left\{\mathbf{X}\right\}\mathbf{F}^L$, which is an $N \times L$ matrix. Therefore, we separate the BEM coefficients out successfully. Thus, we obtain:

$$\mathbf{Y} = \sum_{q=0}^{Q-1} \mathbf{D}_q\boldsymbol{\Delta}_q\mathbf{X} + \mathbf{W} = \sum_{q=0}^{Q-1} \mathbf{D}_q\hat{\mathbf{X}}\mathbf{c}_q + \mathbf{W}\,. \tag{13}$$

And we set:

$$\mathbf{D} = \left[\mathbf{D}_0\hat{\mathbf{X}}, \cdots, \mathbf{D}_{Q-1}\hat{\mathbf{X}}\right] = \left[\mathbf{D}_0, \cdots, \mathbf{D}_{Q-1}\right]\left[I_Q \otimes \hat{\mathbf{X}}\right], \tag{14}$$

where $\mathbf{D}$ is an $N \times LQ$ matrix, and $\otimes$ denotes Kronecker product. Then, we define $\bar{\mathbf{c}} = \left[\mathbf{c}_0^T, \mathbf{c}_1^T, \cdots, \mathbf{c}_{Q-1}^T\right]^T$, which is a $LQ \times 1$ column vector. Consequently, we get the basic equation, which can solve the QL BEM coefficients:

$$\mathbf{Y} = \mathbf{D}\bar{\mathbf{c}} + \mathbf{W}. \tag{15}$$

In order to track fast time-varying channel, we need to insert comb pilot in frequency domain. We arrange M pilot clusters in N subcarriers of OFDM system as shown in Fig. 2. The length of each pilot cluster is $L_p + 2L_z$, where L_p is the number of non-zero pilot subcarriers, L_z represents the number of the pilot subcarriers whose value are zero, and we set L_z is an even number. Then we assume that the length of each data cluster is L_d. And we set $L_p = 1$. We suppose that the ICI comes mainly from a few adjacent subcarriers. In order to avoid the interference between the pilot information and data information, we arrange guard intervals on both sides to protect the non-zero pilots in comb pilot clusters.

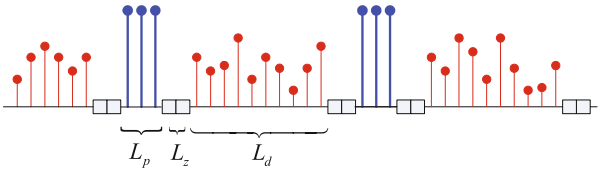

Fig. 2. Comb pilot pattern.

We set $\mathbf{X}_m^{(\mathbf{p})}(m = 0, 1, \cdots, M-1)$ as the m-th pilot cluster. Then, we need to select the appropriate received samples. We can find the corresponding pilot-received signal according to the index value of the pilot directly. Considering that the energy of non-zero pilot subcarriers will spread to a few adjacent subcarriers, we set both the received signal in non-zero pilot subcarriers and half of the received signal in the corresponding guard pilot subcarriers which are more close to non-zero pilot as the received samples. And we assume that L_z is an even number. So, we consider the corresponding pilot-received signal of the m-th sample cluster $\mathbf{Y}_m^{(p)}$ is a $(L_p + L_z) \times 1$ column vector, which can be written as:

$$\begin{aligned}\mathbf{Y}_m^{(p)} &= \sum_{q=0}^{Q-1} \mathbf{D}_{q,m}^{(p)} \hat{\mathbf{X}}^{(p)} \mathbf{c}_q + \sum_{q=0}^{Q-1} \mathbf{D}_{q,m}^{(d)} \hat{\mathbf{X}}^{(d)} \mathbf{c}_q + \mathbf{W}_m \\ &= \sum_{q=0}^{Q-1} \mathbf{D}_{q,m}^{(p)} \hat{\mathbf{X}}^{(p)} \mathbf{c}_q + \mathbf{W}_{d,m} + \mathbf{W}_m^{(p)}\end{aligned}, \tag{16}$$

where $\mathbf{W}_m^{(p)}$ denotes the Gaussian white noise in frequency domain for the m-th sample cluster, and $\mathbf{W}_{d,m}$ indicates the interference between the data subcarriers and the pilot subcarriers. $\mathbf{D}_q^{(p)}$ is an $M(L_p + L_z) \times M(L_p + L_z)$ matrix, which is separated from the corresponding position of the sample subcarriers of $\mathbf{D}_q$. $\mathbf{D}_{q,m}^{(p)}$ is a $(L_p + L_z) \times M(L_p + L_z)$ matrix, which is separated from the corresponding position of the m-th sample cluster of $\mathbf{D}_q^{(p)}$.

Then, we define an $M(L_p + L_z) \times L$ matrix: $\hat{\mathbf{X}}^{(p)}$, which is separated from the corresponding position of the sample subcarriers of $\hat{\mathbf{X}}$. Then, we define two matries:

$$\mathbf{D}_m^{(p)} = \left[\mathbf{D}_{0,m}^{(p)}, \mathbf{D}_{1,m}^{(p)}, \cdots, \mathbf{D}_{Q-1,m}^{(p)}\right], \tag{17}$$

$$\hat{\mathbf{X}}_Q^{(p)} = I_Q \otimes \hat{\mathbf{X}}^{(p)}, \tag{18}$$

where $\mathbf{D}_m^{(p)}$ is a $(L_p + L_z) \times M(L_p + L_z)Q$ matrix, and $\hat{\mathbf{X}}_Q^{(p)}$ is an $M(L_p + L_z)Q \times LQ$ matrix. Therefore, Eq. (16) can be rewritten as: $\mathbf{Y}_m^{(p)} = \mathbf{D}_m^{(p)} \hat{\mathbf{X}}_Q^{(p)} \bar{\mathbf{c}} + \mathbf{W}_{d,m} + \mathbf{W}_m^{(p)}$. Taking all of the sample clusters into account, we define a $(L_p + L_z) M \times M(L_p + L_z)Q$ matrix :

$$\mathbf{D}^{(p)} = \left[\mathbf{D}_0^{(p)T}, \mathbf{D}_1^{(p)T}, \cdots, \mathbf{D}_{M-1}^{(p)T}\right]^T. \tag{19}$$

Finally, we obtain the received signal of the corresponding sample position $\mathbf{Y}^{(p)}$, which can be derived by: $\mathbf{Y}^{(p)} = \mathbf{D}^{(p)}\hat{\mathbf{X}}_Q^{(p)}\bar{\mathbf{c}} + \mathbf{W}_d + \mathbf{W}^{(p)}$, where $\mathbf{W}_d$ indicates the interference between the data subcarriers and the pilot subcarriers, $\mathbf{W}^{(p)}$ represents the Gaussian white noise in frequency domain, and $\mathbf{Y}^{(p)}$ is a $(L_p + L_z)\,M \times 1$ column vector. Therefore, we obtain the basic equation of pilot-assisted channel estimation strategy. Then, we set a $(L_p + L_z)\,M \times LQ$ matrix: $\mathbf{\Omega}^{(p)} = \mathbf{D}^{(p)}\hat{\mathbf{X}}_Q^{(p)}$. Thus, based on LS criterion, we get the estimation of BEM coefficients:

$$\bar{\mathbf{c}} = \left(\mathbf{\Omega}^{(p)}\right)^{-\dagger}\mathbf{Y}^{(p)}, \tag{20}$$

where $\left(\mathbf{\Omega}^{(p)}\right)^{-\dagger}$ denotes the pseudo inverse matrix of $\mathbf{\Omega}^{(p)}$.

4 Simulation Results and Discussions

In this section, we evaluate the performance of P-BEM, DCT-BEM, CE-BEM, GCE-BEM, and OGCE-BEM by simulation. The related simulation parameters are set to $N = 256$, $T_s = 0.5$ μs, $f_c = 2.6$ GHz, and $L = 4$.

According to the system model in this paper, we can find that the propagation path of radio wave contains a line-of-sight (LOS) path and multiple non line-of-sight (NLOS) paths. Thus, we can adopt Rician fading channel model to describe the real channel [14]. We use NMSE to measure the estimation precision of various BEMs. NMSE is defined as:

$$NMSE = \frac{\frac{1}{N}\sum_{n=0}^{N-1}\left|h\left[n\right] - \hat{h}\left[n\right]\right|^2}{\frac{1}{N}\sum_{n=0}^{N-1}\left|h\left[n\right]\right|^2}, \tag{21}$$

where $h(n)$ denotes the impulse response value at the n-th moment of the real channel, $\hat{h}(n)$ is the estimation of the impulse response at the n-th moment. The impulse response of the wireless channel is the sum of L paths at the receiver, so $\hat{h}(n)$ can be represented as $\hat{h}(n) = \sum_{l=0}^{L-1}\hat{h}[n,l]$.

As shown in Figs. 3 and 4, we model the wireless channel by BEMs ($Q = 4$). Then, we adopt the estimation strategy of fast time-varying channel. Next, we regard signal-to-noise ratio (SNR) as a variable in the simulation and set the value range of SNR is [0, 30] dB. It can be seen that the ability of model fitting is getting better as SNR increases. In Fig. 4, the normalized Doppler frequency shift f_d is about 0.12, while the speed of mobile terminal v is 400 km/h. Apart from the similar changing trend of NMSE and SNR, we can observe that the performance of OGCE-BEM is superior to the GCE-BEM on a certain extent. It can be explained that OGCE-BEM effectively reduces the influence of Gaussian white noise and overcomes the problem of spectrum leakage in CE-BEM. In addition, the performance of OGCE-BEM and GCE-BEM are better than DCT-BEM, CE-BEM, and P-BEM obviously while $v = 400$ km/h. In Fig. 3, the speed

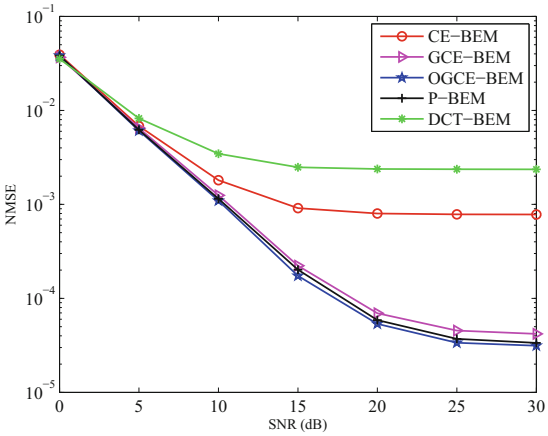

Fig. 3. NMSE versus SNR with $v = 50\,\text{km/h}$.

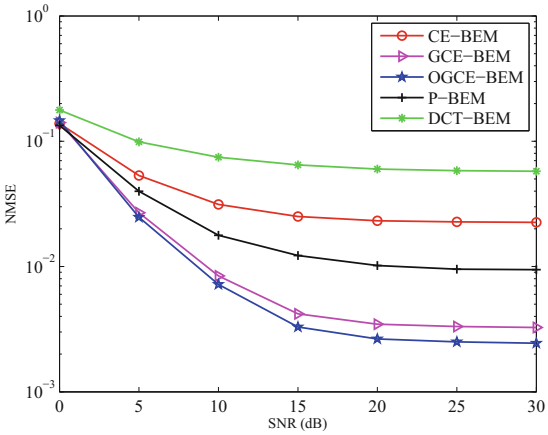

Fig. 4. NMSE versus SNR with $v = 400\,\text{km/h}$.

of mobile terminal v is 50 km/h, the performance of OGCE-BEM is a little better than GCE-BEM and P-BEM, and is much better than CE-BEM and DCT-BEM.

Figure 5 illustrates the relationship between NMSE and the speed of mobile terminal. We set SNR = 20 dB and $Q = 4$. From the figure, we can find that as the speed of mobile terminal increases, the performance of BEMs deteriorates gradually. That is because the speed of mobile terminal is increased continually, which results in an increase in ICI power. Additionally, the capacity of OGCE-BEM and GCE-BEM against the influence of Doppler shift is stronger than P-BEM, DCT-BEM, and CE-BEM visibly. Moreover, the ability of model fitting gets distinctly worse while Doppler shift becomes more and more serious, the reason is that P-BEM and DCT-BEM are sensitive to Doppler shift.

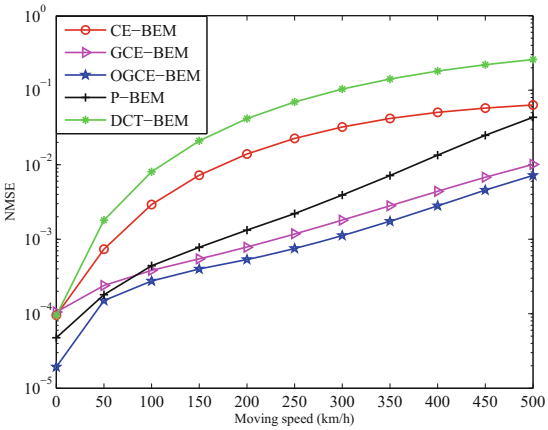

Fig. 5. NMSE versus moving speed with SNR = 20 dB.

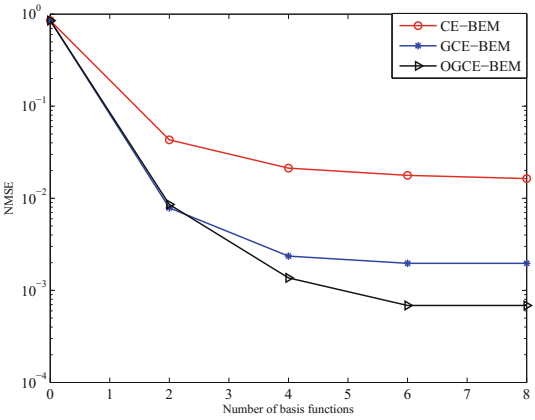

Fig. 6. NMSE versus number of basis functions with SNR = 20 dB and $v = 400$ km/h.

Figure 6 depicts the relationship between NMSE and model order Q while $v = 400$ km/h. We know that the performance of OGCE-BEM and GCE-BEM is better than other BEMs in high speed scenarios, so we focus on OGCE-BEM and GCE-BEM. Observing the similar changing tendency between NMSE and model order, we can find that NMSE decreases as the model order grows from 0 to 8. This is because the BEMs can approximate the real channel more accurately as model order becomes higher. Furthermore, estimation precision of various BEMs has reached a relatively ideal order of magnitude while model order is 6, especially OGCE-BEM. It can be explained that a smaller amounts of BEM basis functions are just enough to match the fast time-varying channel.

5 Conclusion

We investigated the fast time-varying channel estimation strategy in high-speed railway LTE-R communication system. By using BEM, the channel impulse response was expressed as the summation of several basis functions multiplied by the corresponding coefficients. Then, we inserted comb pilot clusters in the frequency domain. Based on the least-square estimation criterion, we achieved the estimation of the channel impulse response by estimating the BEM coefficients, which can reduce the computational complexity significantly. Simulation results verify that BEM can well approximate the fast time-varying channel. Furthermore, OGCE-BEM has a higher estimation precision in different types of BEMs. In order to further reduce the number of pilots, a distributed compressed sensing method will be considered in the future work.

Acknowledgments. This work is supported in part by the National Natural Science Foundation of China (Grant No. U1405251), the Natural Science Foundation of Fujian Province (Grant No. 2015J05122), the Education Department Foundation of Fujian Province (Grant No. JA15089), the Science and Technology Development Foundation of Fuzhou University (Grant No. 2014-XY-30), and the Scientific Research Starting Foundation of Fuzhou University (Grant No. 022572).

References

1. Martin-Vega, F.J., Delgado-Luque, I.M., Blanquez-Casado, F., Gomez, G., Aguayo-Torres, M.C., Entrambasaguas, J.T.: LTE performance over high speed railway channel. In: 78th IEEE Vehicular Technology Conference, pp. 1–5. IEEE Press, Las Vegas (2013)
2. Muneer, P., Sameer, S.M.: Pilot-aided joint estimation of doubly selective channel and carrier frequency offsets in OFDMA uplink with high-mobility users. IEEE Trans. Veh. Technol. **64**, 411–417 (2015)
3. Wang, S., Hu, J.K.: Blind channel estimation for single-input multiple-output OFDM systems: zero padding based or cyclic prefix based? Wirel. Commun. Mob. Comput. **12**, 204–210 (2013)
4. Cagatay, C.: An accurate and efficient two-stage channel estimation method utilizing training sequences with closed form expressions. IEEE Trans. Commun. **59**, 3259–3264 (2011)
5. Coleri, S., Ergen, M., Puri, A., Bahai, A.: Channel estimation techniques based on pilot arrangement in OFDM systems. IEEE Trans. Broadcast. **48**, 223–229 (2002)
6. Mousa, A., Mahmoud, H.: Channels estimation in OFDM system over Rician fading channel based on comb-type pilots arrangement. IET Sig. Proc. **4**, 598–602 (2010)
7. Zhong, K., Lei, X., Li, S.Q.: Wiener filter for basis expansion model based channel estimation. IEEE Commun. Lett. **15**, 813–815 (2011)
8. Tang, Z.J., Cannizzaro, R.C., Leus, G., Banelli, P.: Pilot-assisted time-varying channel estimation for OFDM systems. IEEE Trans. Signal Process. **55**, 2226–2238 (2007)
9. Leus, G.: On the estimation of rapidly time varying channels. In: 12th European Signal Processing Conference, pp. 2227–2230. IEEE Press, Vienna (2004)

10. Huang, C.L., Chen, C.W., Wei, S.W.: Channel estimation for OFDM system with two training symbols aided and polynomial fitting. IEEE Trans. Commun. **58**, 733–736 (2010)
11. Tse, D., Viswanath, P.: Fundamentals of wireless communication. IEEE Trans. Inf. Theory **52**, 919–920 (2009)
12. Stamoulis, A., Diggavi, S.N., Al-Dhahir, N.: Intercarrier interference in MIMO-OFDM. IEEE Trans. Sig. Process. **50**, 2451–2464 (2002)
13. Chiong, C.W.R., Rong, Y., Xiang, Y.: Channel estimation for time-varying MIMO relay systems. IEEE Trans. Wirel. Commun. **14**, 6752–6762 (2015)
14. Beaulieu, N.C., Chen, Y.: Maximum likelihood estimation of local average SNR in ricean fading channels. IEEE Commun. Lett. **9**, 219–221 (2005)